Laser Physics, Vol. 9, No. 1, 1999, pp. 1–10.

Strong-Field Double Ionization of Helium: A Density-Functional Perspective

M. Petersilka and E. K. U. Gross

Institut für Theoretische Physik, Universität Würzburg, Am Hubland, Würzburg, 97074 Germany

e-mail: gross@physik.uni-wuerzburg.de

Received August 31, 1998

Abstract—In this work we address the problem of multiple ionization of atoms in strong laser fields (in the infrared and visible range). To this end we numerically solve the full, three-dimensional time-dependent Kohn–Sham equations for a Helium atom in a strong laser field at wavelengths of 780 and 614 nm. Explicit density functionals for the calculation of ionization probabilities are developed. From the results, we will draw conclusions about the role of electronic correlation in the ionization dynamics and about the validity of present-day exchange-correlation potentials.

1. INTRODUCTION

Owing to the rapid experimental progress in the field of laser physics, ultrashort laser pulses of very high intensities have become available in recent years. The electric field produced in such pulses can reach or even exceed the strength of the static nuclear Coulomb field experienced by an electron on the first Bohr orbit. In the hydrogen atom, this electric field is of the order of 5.1×10^9 V/m, which corresponds to the electric field amplitude of an electromagnetic plane wave of intensity 3.51×10^{16} W/cm^2. If an atom is placed in the focus of such a laser pulse one observes a wealth of novel phenomena [1–3] which cannot be explained by ordinary perturbation theory.

The advent of short laser pulse experiments has revealed evidence of a significantly enhanced production of doubly charged noble gas atoms [4]. Recently, in high-precision measurements covering a wide dynamical range of intensity-dependent ionization [5, 6], a "knee" structure in the double ionization yields of Helium has been observed. Up to an intensity of roughly 3×10^{15} W/cm^2, the double-ionization yields *are orders of magnitude* above the signal that one would expect from a "sequential" mechanism, where the second electron only comes from the ionization of He^+. The He^+ and the He^{2+} curves saturate at the same intensity, indicating that the ionization does proceed nonsequentially.

The salient feature of enhanced double ionization suggests the existence of a "direct" process where the amount of energy absorbed from the radiation field is shared among the two electrons. Needless to say, that the so-called "single-active electron approximation" [7, 8], which is based on the assumption that just one electron at a time is being active in the interaction with the external laser field, is not capable of describing these effects. Perturbative methods [9–11] and the solution of theoretical models based on a simplified dielectronic interaction [12] underline the importance of time-dependent electron–electron correlation during the process. Further evidence of the fact that electron correlation leads to qualitative effects in intense laser–atom interactions was gained from the recent solution of the time-dependent Schrödinger equation of a one-dimensional model atom [13].

The double-ionization measurements constitute the most distinct manifestation of electron correlation in the physics of intense laser–atom interactions, making indispensable a nonperturbative quantum mechanical description of interacting electrons in strong, time-dependent external fields. In principle, this requires the full solution of the three-dimensional time-dependent Schrödinger equation for interacting many-particle systems. Work along these lines for the helium atom has already begun [14–16], but even with the use of modern massively parallel computers, the problem is barely tractable. Clearly, in view of its computational advantages, time-dependent density functional theory [17, 18] opens up a viable route towards the exploration of the physics of time-dependent many-particle systems. It provides an in principle exact alternative to account for the fully correlated character of the problem by virtue of the time-dependent exchange-correlation potential. The solution of the time-dependent Kohn–Sham equations brings within reach a fully nonlinear time-dependent *all electron* treatment of atoms in strong laser fields.

2. INTEGRATION OF THE TIME-DEPENDENT KOHN–SHAM EQUATIONS

By virtue of the theorem of Runge and Gross [17], every observable can, in principle, be calculated from the time-dependent density. In the framework of time-

dependent density functional theory, this density can be obtained from

$$n(\mathbf{r}, t) = \sum_{j=1}^{N} |\varphi_j(\mathbf{r}, t)|^2 \quad (1)$$

(N being the number of electrons) with orbitals $\varphi_{j\sigma}(\mathbf{r}, t)$ satisfying the time-dependent Kohn–Sham equation

$$i\frac{\partial}{\partial t}\varphi_j(\mathbf{r}, t) = \left(-\frac{\nabla^2}{2} + v(\mathbf{r}, t) + \int d^3r' \frac{n(\mathbf{r}', t)}{|\mathbf{r} - \mathbf{r}'|} + v_{\mathrm{xc}}[n](\mathbf{r}, t)\right) \times \varphi_j(\mathbf{r}, t) \quad (2)$$

(atomic units are used throughout). In practice, the time-dependent exchange-correlation potential v_{xc} has to be approximated. The total *external* potential experienced by the electrons in the helium atom (in dipole approximation and length gauge) is given by

$$v(\mathbf{r}, t) = E_0 f(t) z \sin(\omega t) - \frac{2}{r}. \quad (3)$$

The electric field of the laser with frequency ω and peak strength E_0 is assumed to be polarized along the z-direction, and can further be characterized by an envelope function $f(t)$.

Throughout the propagation, the equidistant time-steps were chosen according to $\Delta t \le (4U_{\mathrm{p0}})^{-1}$, with $U_{\mathrm{p0}} = E_0^2/(4\omega^2)$ being the ponderomotive potential at the peak of the pulse.

To avoid spurious reflections at the grid boundary, absorbing boundary conditions are introduced: After each time step, the orbitals are multiplied by a function which is unity on the interior of the grid and then falls to zero like $\cos^{1/4}$ over a width of roughly ten percent of the respective total grid size.

Due to axial symmetry, discretization in cylindrical coordinates leads to a nonuniform rectangular grid in the (ρ, z)-plane. In the z-direction, the dimension of the grid is governed by the classical amplitude $\alpha_{\mathrm{class}} = E_0/\omega^2$ of the quiver motion of an electron in the electric field E_0 at the peak of the pulse. The grid was chosen to include the classical amplitude α_{class} at least 4 times, i.e., $|z| < z_{\max}$ with $z_{\max} > 2\alpha_{\mathrm{class}}$. At the same time, the stepsize Δz cannot be too large, in order to permit propagation of sufficiently large momentum components of the wavefuntion.

The integration of the single-particle equations is performed using the standard finite-difference representation of the kinetic-energy operator. To obtain the ground state density, diagonalization of the Hamilton matrix without external field is performed.

The time-dependent orbitals are labelled by the indices characterizing their initial state: the orbital $\varphi_{1s}(\mathbf{r}, t)$ describes an electron which initially occupied a 1s orbital.

3. DENSITY-FUNCTIONAL APPROACH TO IONIZATION YIELDS

A possible way to define ionization probabilities is by means of a geometrical concept. By dividing the space $\mathbb{R}^3$ into two regions, the analyzing volume A (which has to be appropriately chosen), and its complement $B = \mathbb{R}^3 \backslash A$, the norm of the correlated two-particle wavefunction can be written as

$$1 = \int_A d^3r_1 \int_A d^3r_2 |\Psi(\mathbf{r}_1, \mathbf{r}_2, t)|^2 + 2\int_A d^3r_1 \int_B d^3r_2 |\Psi(\mathbf{r}_1, \mathbf{r}_2, t)|^2 + \int_B d^3r_1 \int_B d^3r_2 |\Psi(\mathbf{r}_1, \mathbf{r}_2, t)|^2 . \quad (4)$$

The second term (AB) in (4) is equal to the probability of finding one electron inside the volume A and simultaneously finding the other electron outside the volume A This is interpreted as single ionization. In analogy, the third term (BB) in (4) is given the interpretation of double ionization. The above interpretation rests on the assumption that (i) those components of the time-dependent wave function which belong to the continuum at the end of the pulse, have propagated away from the nucleus so that their contribution to the norm inside the analyzing volume can be neglected and (ii) that the analyzing volume is large enough so that the bound-state population is well represented by the norm inside A.

Even with the most powerful supercomputers to date, the calculation of the time-dependent, three-dimensional, fully correlated wavefunction remains a computationally extremely demanding task [16].

In the framework of time-dependent density functional theory on the other hand, much of the numerical load can be circumvented because the central equations to be solved, the time-dependent Kohn–Sham equations (1), (2), are only single-particle Schrödinger equations. The basic variable within this scheme, however, is the time-dependent *density* $n(\mathbf{r}, t)$ rather than the time-dependent wave function. The Kohn–Sham determinant, built from the orbitals satisfying equations (1), (2) is solely designed to reproduce the physical density. Besides that, the Kohn–Sham determinant has no rigorous physical meaning. Moreover, due to the nonlinear character of the time-dependent Kohn-Sham equations, the Kohn–Sham determinant lacks the principle of superposition: It is well known from the solution of the time-dependent Hartree–Fock (TDHF) equations, which, in the case of Helium, can be regarded as a special case of the time-dependent Kohn–Sham equations, that stable transition probabilities can usually not be calculated from TDHF wave functions.

The projection of a TDHF wave function on stationary states often gives probabilities oscillating in time even in the absence of an external field.

By virtue of the Runge–Gross theorem, every observable can be expressed as a functional of the density. The key problem is how to construct these functionals in explicit terms. In the special case of two-electron systems, the diagonal of the time-dependent two-particle density matrix is

$$\Gamma(\mathbf{r}_1, \mathbf{r}_2, t) = 2\left|\Psi(\mathbf{r}_1, \mathbf{r}_2, t)\right|^2. \tag{5}$$

The two-particle density matrix in turn is related to the density via the pair-correlation function

$$g(\mathbf{r}_1, \mathbf{r}_2, t) := \frac{\Gamma(\mathbf{r}_1, \mathbf{r}_2, t)}{n(\mathbf{r}_1, t)n(\mathbf{r}_2, t)} \tag{6}$$

which satisfies the important sum rule

$$\int d^3r_2 n(\mathbf{r}_2, t)(g(\mathbf{r}_1, \mathbf{r}_2, t) - 1) = -1. \tag{7}$$

Physically, the product $n(\mathbf{r}_2, t)g(\mathbf{r}_1, \mathbf{r}_2, t)$ is the (conditional) probability to find an electron at $(\mathbf{r}_2, t)$, if we know that there is an electron at $(\mathbf{r}_1, t)$. The crucial point is that the pair-correlation function can, in principle exactly, be expressed as a functional of the density: $g[n](\mathbf{r}_1, \mathbf{r}_2, t)$.

With the pair-correlation function being a functional of the time-dependent density, the expressions for single- and double-ionization probabilities of helium read

$$P^0(t) = \frac{1}{2}\int_A d^3r_1 \int_A d^3r_2 n(\mathbf{r}_1, t)n(\mathbf{r}_2, t)g[n](\mathbf{r}_1, \mathbf{r}_2, t) \tag{8}$$

$$P^{+1}(t) = \int_A d^3r n(\mathbf{r}, t) - \int_A d^3r_1 \int_A d^3r_2 n(\mathbf{r}_1, t)n(\mathbf{r}_2, t)g[n](\mathbf{r}_1, \mathbf{r}_2, t) \tag{9}$$

$$P^{+2}(t) = 1 - \int_A d^3r n(\mathbf{r}, t) + \frac{1}{2}\int_A d^3r_1 \int_A d^3r_2 n(\mathbf{r}_1, t)n(\mathbf{r}_2, t)g[n](\mathbf{r}_1, \mathbf{r}_2, t). \tag{10}$$

In practice, the density functional approach towards the calculation of ionization involves two basic approximations:

(1) The time-dependent density is calculated using some approximate exchange-correlation potential.

(2) The functional dependence of the pair-correlation function g on the density n in (8)–(10) is only approximately known.

3.1. Exact Exchange-Only Limit, Mean-Field Approach

In a "Hartree–Fock world," the exact wave functions of many-particle systems would be Slater-determinants. For Helium, the exact pair-correlation function in this exchange-only limit is simply a constant:

$$g_x[n](\mathbf{r}_1, \mathbf{r}_2, t) = \frac{1}{2}. \tag{11}$$

Substituting the exchange-only pair-correlation function from equation (11) into (8)–(10), the ionization probabilities of helium are given by

$$P^0(t) = N_{1s}(t)^2, \tag{12}$$

$$P^{+1}(t) = 2N_{1s}(t)(1 - N_{1s}(t)), \tag{13}$$

$$P^{+2}(t) = (1 - N_{1s}(t))^2, \tag{14}$$

where we have defined

$$N_{1s} := \frac{1}{2}\int_A d^3r n(\mathbf{r}, t) = \int_A d^3r \left|\phi_{1s}(\mathbf{r}, t)\right|^2. \tag{15}$$

Formulas (12)–(14) could have been obtained directly from (4) by substituting any determinantal wavefunction for the exact wave function Ψ. In particular, approximating the true wave function in a *mean-field* sense by the Kohn–Sham determinant, equations (12)–(14) represent the most straightforward way to extract information about ionization probabilities from a time-dependent Kohn–Sham calculation. However, this notion sacrifices the joint probability character of the two-particle density matrix, and one is left with just an uncorrelated product of single-particle densities.

3.2. Correlation Contributions

The definition of the x-only limit for the pair-correlation function suggests to distinguish between exchange and correlation contributions to the pair-correlation function. Combining the exact exchange expression (11) with the correlation contribution g_c in the density-functional approach (8)–(10), exactifies the mean-field expressions (12)–(14) by adding correlation corrections

$$P^0(t) = N_{1s}(t)^2 + \frac{1}{2}\int_A d^3r_1 \int_A d^3r_2 n(\mathbf{r}_1, t)n(\mathbf{r}_2, t)g_c[n](\mathbf{r}_1, \mathbf{r}_2, t), \tag{16}$$

$$P^{+1}(t) = 2N_{1s}(t)(1 - N_{1s}(t)) - \int_A d^3r_1 \int_A d^3r_2 n(\mathbf{r}_1, t)n(\mathbf{r}_2, t)g_c[n](\mathbf{r}_1, \mathbf{r}_2, t), \tag{17}$$

$$P^{+2}(t) = (1 - N_{1s}(t))^2 + \frac{1}{2}\int_A d^3r_1 \int_A d^3r_2 n(\mathbf{r}_1, t) n(\mathbf{r}_2, t) g_c[n](\mathbf{r}_1, \mathbf{r}_2, t). \quad (18)$$

In the literature, a variety of approximate functionals for the pair correlation function g have been put forward [19–22] which allow for quite accurate calculations of ground-sate properties of many-particle systems [23]. At present, the properties of an explicitly *time-dependent* pair-correlation function are a rather unexplored topic. For the time being, we will thus use existing functionals, developed for stationary systems, in the spirit of an adiabatic approximation: The pair-correlation function at time t is modeled by evaluating the ground-state functional at the time-dependent density:

$$g[n](\mathbf{r}_1, \mathbf{r}_2, t) \approx g^{\text{stat}}[\rho](\mathbf{r}_1, \mathbf{r}_2)\big|_{\rho = n(t)}. \quad (19)$$

Since, for two-electron systems, the exact time-dependent pair-correlation function in the x-only limit is given by equation (11), spatial and temporal nonlocality can be viewed as pure electron correlation effects in these systems.

A pair-correlation function suitable for our calculations can be deduced within the self-interaction correction (SIC) scheme of Perdew and Zunger [24]. For two electrons, only "self-exchange" is present which, in the SIC scheme, is treated exactly. For the correlation contributions, the parametrization of Perdew and Wang [22] was employed.

As a second functional, we tested a coordinate space model for g_c, developed by A.D. Becke [21] (taken at full coupling strength of the electron–electron interaction):

$$g_c^{\text{Model}}[n](\mathbf{r}_1, \mathbf{r}_2) = \frac{(|\mathbf{r}_1 - \mathbf{r}_2| - z_{\uparrow\downarrow}(\mathbf{r}_1)) n(\mathbf{r}_1)}{2(1 + z_{\uparrow\downarrow}(\mathbf{r}_1)) n(\mathbf{r}_2)} F(\gamma|\mathbf{r}_1 - \mathbf{r}_2|), \quad (20)$$

where γ is determined by the sum rule (7). For the damping factor F, analytic approximations like $F_1(x) = \operatorname{sech}(x)$, $F_2(x) = (1 + x)e^{-x}$ or $F_3(x) = e^{-x^2}$ have been chosen. As extension of the original work of Becke, we propose to use a "correlation length" which is inversely proportional to the Hartree potential v_H:

$$z_{\uparrow\downarrow} = \frac{4C_{\uparrow\downarrow}}{v_H}, \text{ with } C_{\uparrow\downarrow} = 0.62. \quad (21)$$

3.3. Approximations for the Time-Dependent Exchange-Correlation Potential in Helium

For the time-dependent exchange-correlation potential occurring in the time-dependent Kohn–Sham equations (1), (2), we have employed the following functionals:

3.3.1. The time-dependent Hartree–Fock (TDHF) potential

For two-electron systems, the exchange potential

$$v_x^{\text{TDHF}}[n](\mathbf{r}, t) = -\frac{1}{2}\int d^3r' \frac{n(\mathbf{r}', t)}{|\mathbf{r} - \mathbf{r}'|} \quad (22)$$

of the restricted Hartree–Fock equations is identical with the *exact* exchange-only potential in a time-dependent Kohn–Sham treatment of helium.

3.3.2. The adiabatic local density approximation

The easiest way to go beyond the exchange-only approximation, is to use the so-called "adiabatic" local density approximation (ALDA). It employs the functional form of the static LDA with a time-dependent density:

$$v_{xc}^{\text{ALDA}}[n](\mathbf{r}, t) = -\left(\frac{3}{\pi} n(\mathbf{r}, t)\right)^{1/3} + v_c^{\text{LDA}}(\rho)\big|_{\rho = n(\mathbf{r}, t)} \quad (23)$$

In the actual calculations, the parametrization of Perdew and Wang [25] was used for the correlation part.

3.3.3. The time-dependent SIC-potential

For the Helium atom, the expression for the time-dependent SIC (TDSIC) exchange-correlation potential reads

$$v_{xc}^{\text{TDSIC}}[n](\mathbf{r}, t) = -\frac{1}{2}\int d^3r' \frac{n(\mathbf{r}', t)}{|\mathbf{r} - \mathbf{r}'|} + \left(v_c^{\text{LDA}}(\rho, \zeta = 0) - v_c^{\text{LDA}}\left(\frac{1}{2}\rho, \zeta = 1\right)\right)\Big|_{\rho = n(\mathbf{r}, t)} \quad (24)$$

(where $\zeta = (n_\uparrow - n_\downarrow)/n$ is the relative spin polarization). Like in TDHF, the exchange part is treated exactly. In the time-dependent calculations, the correlation potential was evaluated using the parametrization of Perdew and Wang [25].

3.3.4. A model potential

To obtain a correlation potential with a nonlocal functional dependence on the density, we start out from the (coupling-constant averaged) expression of the correlation energy which results from the model correlation hole of equation (20) [21]:

$$E_c^{\text{Model}} = -0.8\int d^3r n(\mathbf{r})^2 z_{\uparrow\downarrow}^2 \left[1 - \frac{\ln(1 + z_{\uparrow\downarrow}^2)}{z_{\uparrow\downarrow}}\right]. \quad (25)$$

With expression (21) proposed here, the resulting correlation potential

$$v_c^{\text{Model}}[n](\mathbf{r}) = -0.4n(\mathbf{r})z_{\uparrow\downarrow}^2\left[1-\frac{\ln(1+z_{\uparrow\downarrow}^2)}{z_{\uparrow\downarrow}}\right] + 0.8C_{\uparrow\downarrow}\int d^2(r')\frac{\dfrac{z_{\uparrow\downarrow}(1+2z_{\uparrow\downarrow})}{1+z_{\uparrow\downarrow}}-\ln(z_{\uparrow\downarrow})}{v_H(\mathbf{r}')^2|\mathbf{r}-\mathbf{r}'|} \quad (26)$$

exhibits a truly nonlocal functional dependence on the density. In combination with exact exchange (22), this forms a self-interaction free exchange-correlation potential v_{xc}^{Model} for the helium atom. The only extra effort in using this potential consists in an additional evaluation of a Coulomb-type integral in (26). For the ground state of helium, this functional yields an eigenvalue and a correlation energy which are very close to the exact DFT values [26]. In the time-dependent case, v_{xc}^{Model} is evaluated at the time-dependent density.

4. IONIZATION OF HELIUM IN A 780-nm FIELD

We have calculated the ionization probabilities for Helium using a 6-cycle laser pulse of frequency ω = 0.0584 a.u. (1.6 eV) with a trapezoidal envelope function: the envelope function in (3) was linearly ramped from zero to one over the first two cycles, held constant for the following two laser cycles and finally ramped down linearly over the last two cycles of the pulse. The peak intensities vary between 2×10^{14} W/cm^2 and 1.14×10^{16} W/cm^2.

Due to the high ponderomotive energy of the electron, a resolution of up to 11000 time steps per optical cycle is needed. For all runs, the boundaries of the cylindrical analyzing volume A were fixed at $-z_A = z_A = \rho_A = 20$ a.u.[1]

The intensity-dependent probability for single ionization of helium obtained from the mean-field expressions (12)–(14) at the end of the pulse is displayed in Fig. 1. For all four approximations to the exchange-correlation potential $v_{xc}(\mathbf{r}, t)$, the probability for singly ionized helium reaches its maximum of 0.5 around an intensity of 4×10^{15} W/cm^2. The subsequent decrease in probability is typical of the single-atom response. Then the He^+ population is depleted in favor of the doubly charged ion production. In current experiments, this behavior is not resolved owing to the spatial intensity profile of the laser focus [27], which gives rise to a monotonic increase of the ion yield due to the expansion of the focal volume.

[1] This choice is arbitrary, but the results are not very sensitive to this choice. For a choice of $-z_{A\,\min} = z_{A\,\max} = \rho_A = 10$ a.u. the results differ only slightly, due to the small percentage of the population in the range between 10 a.u. to 20 a.u.

In our calculations, the saturation intensity tends to be shifted towards higher intensities for two reasons: First, the pulse lengths employed are roughly a factor of 10 shorter than the experimental pulses. A lower saturation intensity occurs when the pulse is longer. Second, the binding energy of the initial finite-difference orbital is elevated by 4% compared to that of the true helium ground state.

Below the saturation intensity, the single-ionization probabilities from Fig. 1 comply with the eigenvalues of the initial orbitals. Due to the local approximation of the exchange contribution, the LDA ground-state orbital is much more weakly bound than in the remaining approximations. Hence, the ionization probabilities in ALDA (23) are significantly larger than the probabilities obtained in TDHF (22), TDSIC (24) and from the model potential (26).

The intensity-dependent *double*-ionization probabilities, calculated from the mean-field equation (14) at the end of the pulse are given in Fig. 2. Compared to the calculated ionization probability from the ground-state of the He^+ ion (SEQ), we observe an enhanced probability for the production of doubly charged ions from the ground state of the neutral He atom.

For high intensities, the double-ionization curve has to merge with the single-ionization from the ground state of He^+, since, in the saturation region of the He^+ yield (i.e., after an almost complete depletion of neutral helium in the focus) the He^+ ion becomes the dominating source for the production of doubly ionized species. In the literature, this notion has been termed a "sequential" process (SEQ). Strictly speaking, no clear definition of a "sequential" or "nonsequential" process is possible due to the indistinguishability of electrons. Both electrons are active at the same time. Experimentally, on the other hand, one only observes a final degree of ionization after the laser-atom interaction has died off.

However, independent of the choice of the exchange-correlation potential, the calculated probabilities are too high for the intensities beyond the maximum of the single ionization probability. Hence, the calculations do not reproduce the famous "knee" structure which is observed in the double-ionization yield of helium in the experiment of Walker *et al.* [6]. Below the intensity of 4×10^{15} W/cm^2, the double-ionization probabilities are again highest in ALDA, followed by quite some interval by the results of the model potential, which are again close to the TDHF results. At higher intensities, both the TDHF and the MODEL curve merge with the TDSIC curve. Interestingly, around $I = 4 \times 10^{15}$ W/cm^2—at the maximum of the single-ionization probabilities—the ALDA-results cross the results from the other, self-interaction free potentials, resulting in a *lower* ionization probability than obtained with the remaining three potentials. But, despite this somewhat lower probability in that inten-

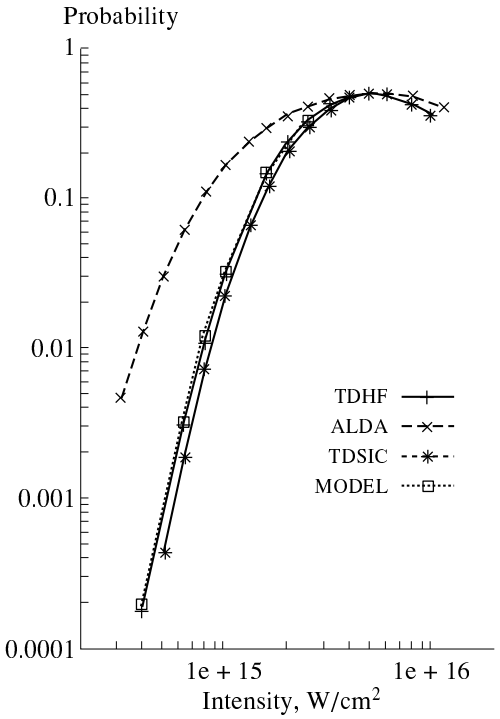

Fig. 1. Calculated He^+ ion probabilities from the ground state of the Helium atom irradiated by a 6-cycle (16 fs), 780-nm laser pulse, using equation (13) and for different exchange-correlation potentials (see text).

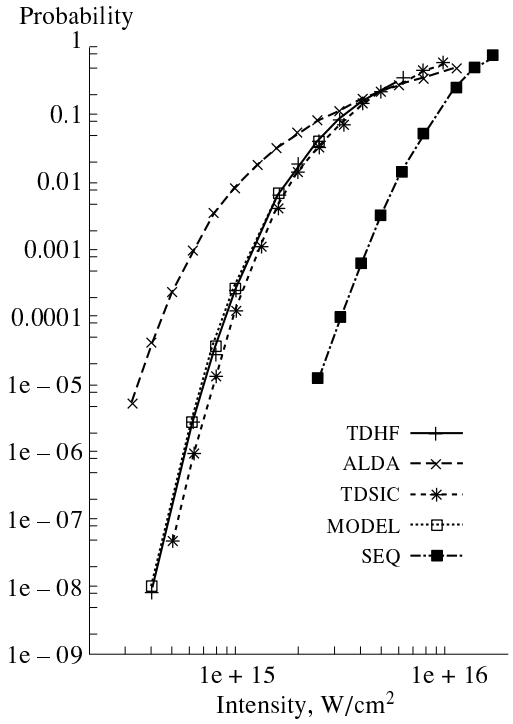

Fig. 2. Calculated double-ionization probabilities from the ground state of the Helium atom irradiated by a 6-cycle (16 fs), 780-nm laser pulse, using equation (14) and for different exchange-correlation potentials (see text).

sity region, the ALDA results are still far from reproducing a "knee" structure.

A decisive measure for the ionization dynamics is provided by the ratio of double-ionization yields to single-ionization yields. The He^{2+}/He^+ ratio of the experimental data [6] varies by about a factor of 10 for intensities between 10^{14} and 10^{15} W/cm^2, and exhibits a distinctly marked plateau (with an experimental value of about 0.002) which extends up to the onset of "sequential" He^{2+} production. In Fig. 3 we have compiled the ratios of the double-ionization probabilities to single ionization probabilities calculated for the different exchange-correlation potentials employed. In contrast to experiment, the ratios show a variation of about 4 orders of magnitude, and a lack of any plateau structure. Hence, compared to experiment, the calculated double-ionization probabilities are too small for low intensities, but too large for higher intensities. The situation is a bit less severe in ALDA. The ratios calculated in ALDA intersect with those obtained in the remaining approximations at the intensity where the single-ionization yields have their maximum (4×10^{15} W/cm^2). Evidently, the functionals employed are not able to reproduce the features present in the strong-field double ionization of helium.

So far, our analysis was entirely based on the mean-field expressions (13) and (14) for the ionization probabilities. To go beyond this limit, we use the concept of the pair-correlation function of Section 3.

The SIC pair-correlation function [24] as well as the coordinate space model (20) treat the exchange hole of helium exactly, thus conserving the bulk of information already contained in the uncorrelated equations (12)–(14), leading to corrections around the mean-field description. The resulting ionization probabilities are then given by the expressions (17) and (18). To this end, we examine the correlation correction

$$\int_A d^3r_1 \int_A d^3r_2 n(\mathbf{r}_1, t) n(\mathbf{r}_2, t) g_c[n](\mathbf{r}_1, \mathbf{r}_2) \qquad (27)$$

evaluated at the densities obtained from a TDSIC calculation for various peak intensities at the end of the 6-cycle, 780-nm pulse.

If the system is only weakly ionized, the density is still concentrated around the nucleus, and, owing to the sum rule (7) a rather small value of the integral (27) is expected. At higher intensities, the highly excited density becomes more diffuse and, due to the finite volume effects, the contribution from (27) increases in magnitude. A countercurrent effect is the decrease of the norm inside A. Hence, as a function of intensity, we

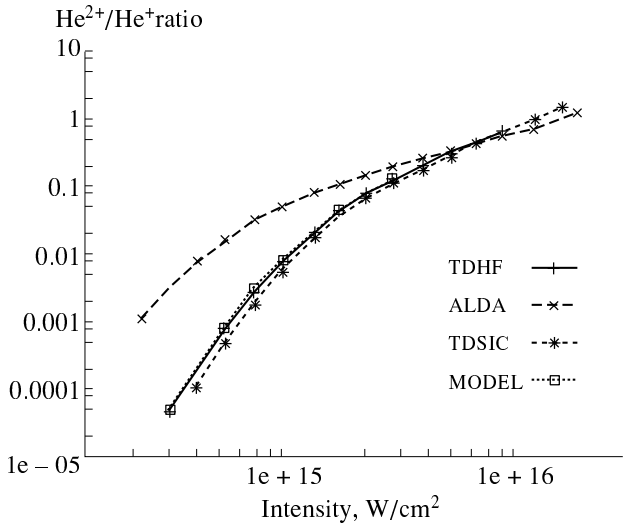

Fig. 3. Comparison of the ratios of double-ionization probability to single-ionization probability calculated from equations (13) and (14) for helium in a 780-nm laser field using the TDHF, ALDA, TDSIC and the Model potential.

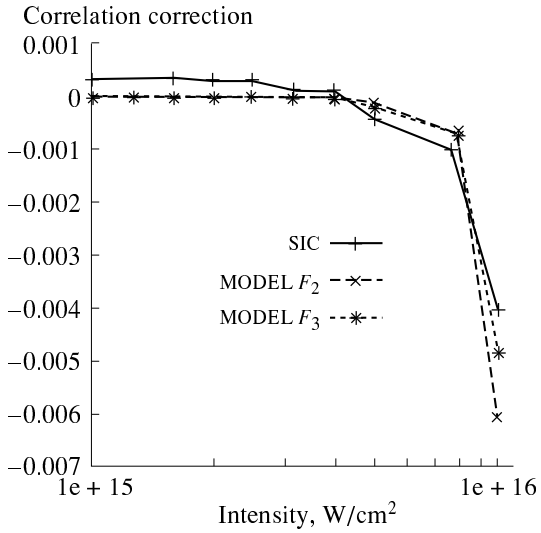

Fig. 4. Correlation corrections (27) to the mean-field equations (12)–(14), evaluated for final densities at various intensities, using three different approximations to the correlation hole (see text). The densities were obtained from a TDSIC calculation.

expect the correlation contribution (27) to possess an extremum.

From Fig. 4, all three approximations to the correlation correction agree within an order of magnitude. The two model correlation holes give an almost vanishing correction for low intensities. The correction obtained from the SIC pair-correlation function exhibits a marked change in sign. This is in accordance with our anticipation from the plot of the He^{2+}/He^{+} ratio. However, although the resulting corrections point in the right direction, they are still too small to account for a visible correction in the ionization spectra.

4.1. Ionization of Helium in a 614-nm Field

The first experimental evidence of a "knee" structure of the He^{2+} ion yield in the intensity region around 10^{15} W/cm^2 was found at a wavelength of 614 nm [5].

At this wavelength, a free electron acquires about 38% less ponderomotive energy (at the peak of the pulse) compared to the 780 nm case, which somewhat mitigates the numerical effort involved in a numerical propagation of the Kohn–Sham orbitals. We solved the time-dependent Kohn–Sham equation (2) using a $\sin^2$-pulse envelope

$$f(t) = \sin^2\left(\frac{\pi}{T}t\right) \qquad (28)$$

with $T = 58$ optical cycles (120 fs) of the external field of frequency $\omega = 0.0742$ a.u. (2 eV) for peak intensities between 5×10^{14} W/cm^2 and 9×10^{15} W/cm^2. The maximum temporal resolution was 2000 time steps per optical cycle. For the exchange-correlation potential, the time-dependent SIC functional of equation (24) was employed.

Using a relatively long pulse length, the maximum of the calculated ionization probability of He^{+} is expected to be close to the experimentally observed saturation of the He^{+} ion yield.

In Fig. 5 we give probabilities for singly and doubly ionized helium, calculated from equations (13) and (14) after the pulse has been turned off.

The single ionization probability reaches its maximum around an intensity of 3×10^{14} W/cm^2. By comparing the calculated double ionization probabilities with the probability for single ionization out of the ground state of He^{+}, we observe that the obtained double ionization probabilities are too large in the region above 3×10^{14} W/cm^2. Apparently, the experimentally measured feature of a "knee" in the He^{2+} yield as a function of intensity is again missing. Also, the plot of the ratios of double ionization probability to single ionization probability, shown in Fig. 6 reveals a strong variation of about 4 orders of magnitude, without any clear sign of the onset of a plateau region.

We also calculated the correlation corrections (27) to the mean-field results of the ionization probabilities (13) and (14). The resulting corrections, using the correlation hole (20) with three different damping functions F_i (see Section 3.2), evaluated with the density at the end of the 614-nm pulse, are given in Fig. 7. Again, the corrections are too small to give a visible correction to the ionization probabilities obtained from the uncorrelated expressions (13) and (14). Nevertheless, around an intensity of 3×10^{14} W/cm^2, near the maximum probability for He^{+} production, a marked increase in

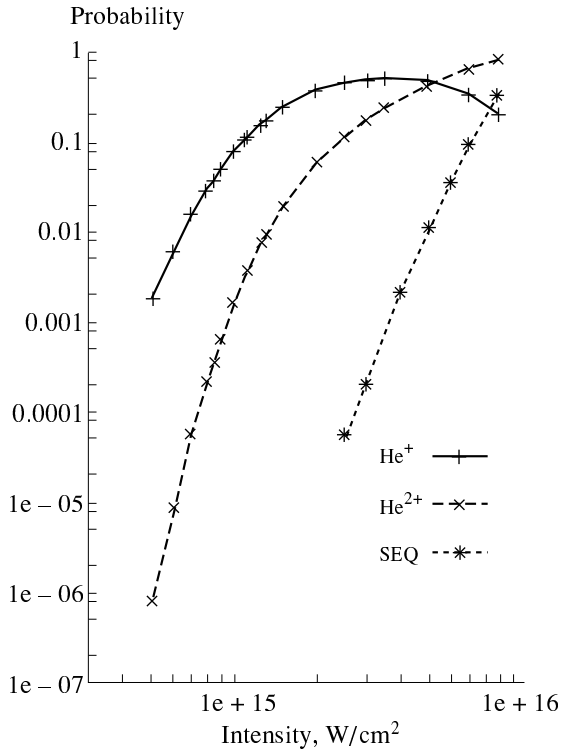

Fig. 5. Calculated probabilities for single ionization (full line) and double ionization (dashed line) from the ground state of the Helium atom irradiated by a 58-cycle (120 fs), 614-nm laser pulse, using equations (13) and the TDSIC exchange-correlation potential. The dotted line represents the ionization probability out of the ground state of the He^+ ion (SEQ).

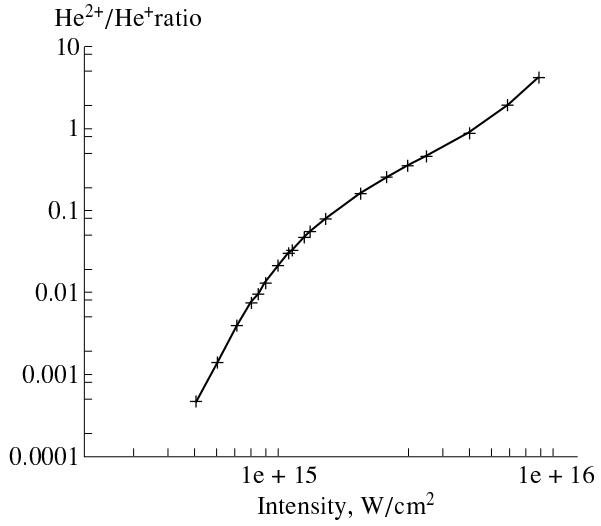

Fig. 6. Ratios of double-ionization probability to single-ionization probability at various intensities, calculated from equations (13) and (14) for helium in a 614-nm laser field using the TDSIC exchange-correlation potential.

magnitude sets in, reducing the double ionization probability.

5. DISCUSSION

Obviously, the approximations to the correlation functionals used are yet not sufficiently accurate to reproduce the typical "knee" feature in the ionization spectrum of helium at 780 and 614 nm. The different sources of error in question are (i) the approximate exchange-correlation potentials used in the Kohn–Sham equation (2) and (ii) the approximate pair-correlation factors entering expressions (12)–(14).

To provide a rationale for the latter, we note that

(1) The modeling of a correlation factor, being at the heart of the quantum many-body problem, is a formidable task even for the ground state of many electron systems. Arbitrarily accurate and, at the same time, universal correlation factors are not available to date.

(2) Most approximations to the correlation factors explicitly require the evaluation of the sum rule (7) during the calculation. However, such a prescription is barely numerically tractable in the case of ionization studies, since it involves numerical integrations over very large grids.

(3) Approximations which circumvent this problem, are mostly based on the homogeneous electron gas and are geared to a good representation of the *spherical average* of the exchange-correlation hole. In particular, this applies to the LDA. Nevertheless, also improved functionals like the SIC [24] and the real-space model of equation (20) only provide an approximation to the angular average of the hole function around some reference point.

(4) The application of even the best available *ground-state* functional to such highly excited systems like an atom in a strong laser pulse has its obvious limitations.

(5) Strictly speaking, one has to use explicitly time-dependent correlation factors $g_c[n](\mathbf{r}, \mathbf{r}', t)$, which are capable of dealing with highly excited states also in a nonperturbative situation. Moreover, explicitly time dependent correlation factors should account for memory effects, i.e., the correlation factor $g_c(t)$ at time t is determined not only by the density $n(t)$ at the same point in time but depends on the density values $n(t')$ at all previous times $t' \le t$. Such memory effects are completely neglected in the present adiabatic treatment.

Another quantity which has to be approximated in a density functional approach is the exchange-correlation potential v_{xc}. The comparison between the (mean-field) ionization probabilities in ALDA with the ionization probabilities calculated from the other functionals reveals that the time-dependent density—and hence the whole dynamics of the system—can be strongly influenced by the choice of the exchange-correlation potential. After all, it is the density which determines the ionization probability.

For a one-dimensional model atom with a softened Coulomb interaction, Lappas and van Leeuwen have solved the full time-dependent Schrödinger equation including an external 780 nm laser field [13]. Their results are reproduced in Fig. 8. From the two-particle wavefunction, they were able to reproduce the "knee" structure in the double ionization probability of helium. Even if the corresponding exact densities of the one-dimensional model system are inserted in the mean-field equations (13) and (14), a distinct, although shifted "knee" structure is still visible in the intensity dependent ionization probability. This suggests that an improved approximation of the exchange-correlation potential alone will account for the qualitative essence of the "knee" feature. However, we note from Fig. 8 that the double ionization probabilities, which result from the insertion of the exact 1-dim densities into the mean-field expressions (13) and (14), are too high by about a factor of four in the plateau region. Thus, in comparison to time-dependent Hartree–Fock, the influence of the exchange-correlation potential and the pair-correlation factors is equally important on a quantitative measure.

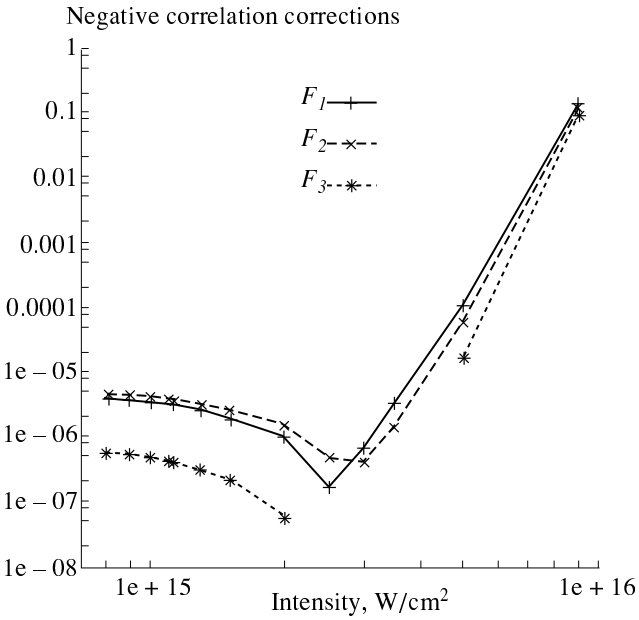

Fig. 7. Negative correlation corrections (27) to the mean-field equations (12)–(14), evaluated for the densities at the end of the 614-nm pulse at various intensities, using the model correlation hole function (20) with three different damping functions. (For intensities between 3×10^{14} W/cm^2 and 5×10^{14} W/cm^2, the corrections obtained with the Gaussian damping function, F_3, change sign and are hence omitted in the figure.)

6. SUMMARY AND CONCLUSION

The results of our simulations have confirmed that the time-dependent Hartree–Fock approximation, which neglects electron correlation, fails to reproduce the correct ionization dynamics of helium. In principle, time-dependent density functional theory offers a possibility to include these correlation effects in a numerically tractable way. In this work, we presented the first density functional study of multiple multiphoton-ionization of helium in strong laser fields. In our calculations, the wavelengths of the incident radiation were chosen to be 780 and 614 nm, according to the experimental situation [5, 6]. Functionals are constructed which allow the calculation of ionization probabilities from the time-dependent density alone. To this end two basic approximations are involved: (i) the time-dependent exchange-correlation potential and (ii) the time-dependent pair correlation function need to be approximated. As a matter of fact, it turned out that the established *stationary* correlation functionals, which were employed in the spirit of an adiabatic approximation, are not sufficient to correct for the defects of the TDHF approximation. A large part of the correlation error (at the frequencies considered here) is already contained in the time-dependent densities. Hence, to obtain a qualitatively correct dynamics, the (time-dependent) exchange-correlation potential needs to be improved in the first place. Even a correlation potential which depends nonlocally on the density, and which reproduces the ground-state properties of helium almost exactly [26] leads only to a marginal improvement over the Hartree–Fock results in the time-dependent case. Hence, for a proper description of time-dependent strong-field phenomena (in the optical region) with the

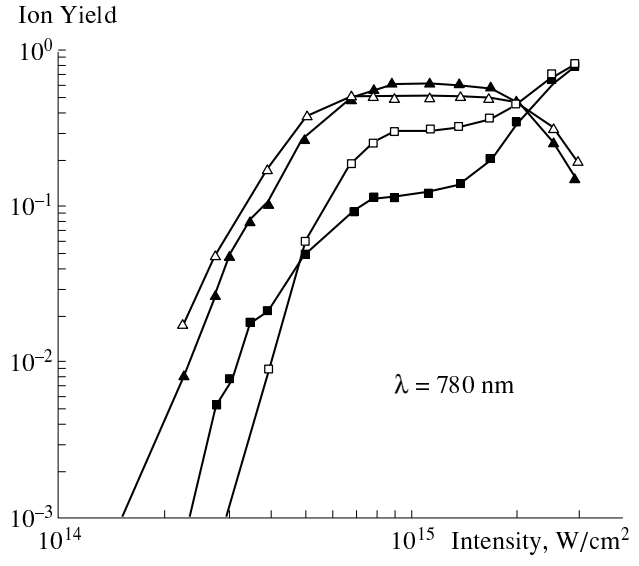

Fig. 8. Single (filled triangles) and double (filled squares) ionization probabilities of a fully correlated one-dimensional helium atom when irradiated by a 780-nm 6-cycle laser pulse. The results from insertion of the exact one-dimensional densities in the mean-field equations (13) and (14) are represented by empty triangles and squares (taken from [13]).

density $n(r, t)$ as a basic variable, highly nonlocal functionals (both spatially and temporally) are required. The first nonlocal functionals of this kind were recently proposed [28, 29], but so far not implemented in time-dependent Kohn–Sham calculations.

ACKNOWLEDGMENTS

Many helpful discussions with T. Kreibich, D.G. Lappas, R. van Leeuwen, and C.A. Ullrich are greatfully acknowledged. This work was supported by the Deutsche Forschungsgemeinschaft.

REFERENCES

1. 1996, in *Super Intense Laser–Atom Physics IV*, vol. 13 of *NATO ASI Series*, Muller, H.G. and Fedorov, M.V., Eds. (Dordrecht: Kluwer).
2. 1997, in *Multiphoton Processes 1996*, no. 154 in *Institute of Physics Conference Series*, Lambropoulos, P. and Walther, H., Eds. (Bristol: Institute of Physics).
3. Protopapas, M., Keitel, C.H., and Knight, P.L., 1997, *Rep. Prog. Phys.*, **60**, 389.
4. L'Huillier, A., Lompre, L.A., Mainfray, G., and Manus, C., 1983, *J. Phys.*, 44, 1247.
5. Fittinghoff, D.N., Bolton, P.R., Chang, B., and Kulander, K.C., 1992, *Phys. Rev. Lett.*, **69**, 2642.
6. Walker, B., Sheehy, B., DiMauro, L.F., *et al.*, 1994, *Phys. Rev. Lett.*, **73**, 1227.
7. Krause, J.L., Schafer, K.J., and Kulander, K.C., 1992, *Phys. Rev. Lett.*, **68**, 3535.
8. Krause, J.L., Schafer, K.J., and Kulander, K.C., 1992, *Phys. Rev. A*, **45**, 4998.
9. Becker, A. and Faisal, F.H.M., 1996, *J. Phys. B*, **29**, L197.
10. Faisal, F.H.M. and Becker, A., 1997, *Laser Phys.*, **7**, 684.
11. Becker, A. and Faisal, F.H.M., 1998, *Laser Phys.*, **8**, 69.
12. Watson, J.B., Sanpera, A., Lappas, D.G., *et al.*, 1997, *Phys. Rev. Lett.*, **78**, 1884.
13. Lappas, D.G. and van Leeuwen, R., 1998, *J. Phys. B*, **31**, L249.
14. Lambropoulos, P. and Tang, X., 1992, in *Atoms in Intense Laser Fields*, Gavrila, M., Ed. (Boston: Academic).
15. Parker, J., Taylor, K.T., Clark, C.W., and Blodgett-Ford, S., 1996, *J. Phys. B*, **29**, L33.
16. Taylor, K.T., Parker, J.S., Dundas, D., and Vivito, S., 1997, in *Multiphoton Processes 1996*, no. 154 in *Institute of Physics Conference Series*, Lambropoulos, P. and Walther, H., Eds. (Bristol: Institute of Physics), p. 56.
17. Runge, E. and Gross, E.K.U., 1984, *Phys. Rev. Lett.*, **52**, 997.
18. Gross, E.K.U., Dobson, J.F., and Petersilka, M., 1996, in *Density Funcional Theory II*, vol. 181 of *Topics in Current Chemistry*, Nalewajski, R.F., Ed. (Berlin: Springer), p. 81.
19. McWeeny, R., 1989, *Methods of Molecular Quantum Mechanics* (London: Academic).
20. Dreizler, R.M. and Gross, E.K.U., 1990, *Density Functional Theory, An Approach to the Quantum Many-Body Problem* (Berlin: Springer).
21. Becke, A.D., 1988, *J. Chem. Phys.*, **88**, 1053.
22. Perdew, J.P. and Wang, Y., 1992, *Phys. Rev. B*, **46**, 12947.
23. Tobias Grabo and Gross, E.K.U., 1995, *Chem. Phys. Lett.*, **240**, 141; erratum: *ibid.* **241**, 635.
24. Perdew, J.P. and Zunger, A., 1981, *Phys. Rev. B*, **23**, 5048.
25. Perdew, J.P. and Wang, Y., 1992, *Phys. Rev. B*, **45**, 13244.
26. Petersilka, M., 1998, *PhD Thesis* (Universität Würzburg).
27. L'Huillier, A., Lompré, L.A., Mainfray, G., and Manus, C., 1983, *Phys. Rev. A*, **27**, 2503.
28. Dobson, J.F., Bünner, M.J., and Gross, E.K.U., 1997, *Phys. Rev. Lett.*, **79**, 1905.
29. Vignale, G., Ullrich, C.A., and Conti, S., 1997, *Phys. Rev. Lett.*, **79**, 4878.